International Journal of Computational and Experimental Science and ENgineering (IJCESEN)

Vol. 12-No.2 (2026) pp. 1-10
http://www.ijcesen.com

Research Article

ISSN: 2149-9144

Application of chitosan beads as an effective biosorbent for orange G dye: characterization, optimization, and Equilibrium Studies

Mohammed Adel Mesbahi[1], Ammar Zobeidi[2.3.*], Belgacem Souyei[4], Nassima Meftah[5], Ahmed Mehellou[6]

[1] Laboratory of Applied Chemistry and Environment (LCAE). Faculty of Exact Sciences. University of El Oued. 39000 El Oued. Algeria.
Email: mohammedadel-mesbahi@univ-eloued.dz- **ORCID:** 0000-0001-5127-2186

[2] Department of Chemistry. Faculty of Exact Sciences. University of El Oued. PO Box 789. El-Oued 39000. Algeria.

[3] Pollution & Waste Treatment Laboratory (PWTL). University of Ouargla. PO Box 511. Ouargla 30000 Algeria.
* **Corresponding Author Email:** zobeidi-ammar@univ-eloued.dz, **ORCID:** 0000-0001-9003-5175

[4] Laboratory of Applied Chemistry and Environment (LCAE). Faculty of Exact Sciences. University of El Oued. 39000 El Oued. Algeria.
Email: belgacem3963_alg@yahoo.fr - **ORCID:** 0000-0002-3564-8910

[5] Laboratory of Applied Chemistry and Environment (LCAE). Faculty of Exact Sciences. University of El Oued. 39000 El Oued. Algeria.
Email: kushal.kanwar@juitsolan.in - **ORCID:** 0000-0001-7646-8572

[6] Laboratory of Applied Chemistry and Environment (LCAE). Faculty of Exact Sciences. University of El Oued. 39000 El Oued. Algeria.
Email: a.mehellou@yahoo.fr - **ORCID:** 0000-0002-9587-440X

Article Info:

DOI: 10.22399/ijcesen.5104
Received : 25 January 2026
Revised : 28 March 2026
Accepted : 01 April 2026

Keywords

Chitosan,
Orange G dye,
Box-Behnken design,
Adsorption.

Abstract:

Chitosan beads (CTS) were prepared and studied in a batch mode operation for the adsorption of Orange G (OG) dye from aqueous solution. Characterization of the surface of CTS was achieved by using point of zero charge (pH_{pzc}) method, Fourier transform infrared spectroscopy, and scanning electron microscopy. The effect of parameters such as adsorbent dosage (A: 0.02-0.06 g), pH (B: 4-10), time of contact (C: 5-45 min), and temperature (D: 30-60°C) on the color removal of OG was investigated using response surface methodology (RSM) based on Box–Behnken surface statistical design at an initial OG concentration, Co = 100 mg/L as a fixed input parameter. Results revealed that the highest removal (92.14 %) of OG dye was achieved by CTS at adsorbent dosage of 0.04g, solution of pH 4, temperature of 60 °C, and time of 25 min. The adsorption process followed the pseudo-second order (PSO) kinetic, and Freundlich isotherm models. The maximum adsorption capacity of CTS composite for OG dye was recorded to be 416.67 mg/g at 60 °C. This work introduces CTS as an ideal composite adsorbent for removal of textile dyes from the aqueous environment.

1. Introduction

Wastewater from textile industries contains synthetic dyes that are toxic, non-biodegradable, and environmentally harmful [1, 2]. When released into water bodies, these dyes block sunlight and reduce oxygen levels, severely disrupting photosynthesis and aquatic life [3]. Several physicochemical methods, including advanced oxidation, coagulation, membrane filtration, and photocatalytic degradation, have been employed for dye removal [4-6]. Among these, adsorption is recognized as a superior technique due to its high efficiency, operational simplicity, cost-effectiveness, and the potential for adsorbent regeneration without generating harmful by-products [7, 8]. Activated carbon offers superior dye adsorption capacity thanks to its porous structure and high surface area, its high cost has prompted research into low-cost, local biosorbents [9]. Among various biosorbents, chitosan (CTS)—a linear polysaccharide derived from the deacetylation of chitin—has garnered significant research attention [10]. Its appeal lies in its biodegradability, non-toxicity, and biocompatibility, but most importantly, its abundant amino ($-NH_2$) and hydroxyl (-OH) functional groups serve as highly effective active sites for pollutant binding [11]. Physical modification of chitosan into forms such as beads, films, or

membranes is essential for improving its adsorptive capacity. This process increases porosity and surface area, allowing better access to internal binding sites [12]. Additionally, it expands the polymer network, enhancing the diffusion of large molecules and reducing the polymer's crystallinity [13]. Reactive azo dyes, characterized by one or more azo bonds (-N=N-) in their molecular structure, represent a large and problematic class of these colored pollutants [14, 15]. Orange G (OG) dye is a common anionic azo dye widely used in the textile industry. Its presence in water streams is highly undesirable, necessitating effective treatment before discharge [16].

Traditional optimization strategies, which rely on varying one parameter while holding others constant, are inherently limited in their ability to reveal the combined effects of multiple variables [17]. To overcome this, response surface methodology (RSM) has been adopted as a powerful statistical tool. RSM not only improves decolorization outcomes but also significantly reduces experimental cost, time, and variability by generating comprehensive data from a limited number of runs [18]. Accordingly, this study utilizes a three-level Box–Behnken design (BBD) to develop chitosan beads (CTS) as an effective biosorbent for reactive dye removal. The effect of operational parameters such as adsorbent dosage, time of contact, temperature, and pH of CTS beads for the removal of OG dye was evaluated and optimized. Orange G (OG) was chosen as a model pollutant because it facilitates electrostatic interaction between the polymer chain and the negatively charged anionic dye.

2. Materials and Methods

2.1. Chemicals and materials

Chitosan (CTS) flakes (deacetylation $\geq$75%; medium MW). Orange G dye ($C_{16}H_{10}N_2Na_2O_7S_2$, MW: 452.37g/mol, λ_{max} = 481 nm) were supplied from Sigma-Aldrich. Hydrochloric acid (HCl. 37%), hydrogen peroxide (H_2O_2), sodium hydroxide (NaOH), and acetic acid (CH_3COOH. 95%) were purchased from Merck (Germany). All experiments of this research were performed using ultrapure water. The molecular structure of GO dye is shown in Fig. 1.

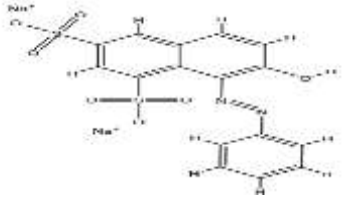

Figure 1. *Molecular structure of Orange G (OG) dye.*

2.2. Preparations and characterization of CTS

The synthesis steps of CTS beads were carried out based on our previous work with some modifications[19, 20]. The 3grams of chitosan flakes was dissolved in 100 mL of 5% acetic acid solution. The viscous solution of chitosan was left with vigorous stirring using a magnetic bar for 24 h until all the chitosan flakes were completely dissolved. The beads were formed by dropping the viscous chitosan solution using a 10 mL syringe (TERUMO 10 cc/mL) into 500 mL of 1 M NaOH solution, and the beads were left stirring for 24 h. The beads were washed using distilled water and dried for 24 h at room temperature; the sample was dried inside an oven at 80° C for 24 h before being ground into a constant particle size $\leq$ 250 µm. The scanning electron microscope and Energy Dispersive X-ray (SEM-EDX) (SEM. Zeiss Supra 40 VP. Germany) was carried out to analyze the surface morphology of CTS before and after OG dye adsorption. The zero point of charge (pH_{pzc}) of the CTS is determined according to the method described in the literature [5].The elemental composition of CTS was determined by using CHNS-O Analyzer (Flash 2000. Organic Elemental Analyzer. Thermo-scientific. Netherlands). Fourier Transform Infrared (FTIR) spectrometer (Cary 600 series. Agilent technologies) was employed to identify the functional groups of CTS before and after OG adsorption.

2.3. Design of Experiments

RSM-BBD was applied for optimizing and studying the impact of four adsorption key factors such as adsorbent dose (A), time (B), temperature (C), and solution pH (D) for the OG dye adsorption onto CTS. The Design Expert 12.0 (Stat-Ease. Minneapolis, USA) software was used as a statistical tool for designing the experiments and performing statistical analysis. Table 1 presents the levels of independent adsorption key factors applied in BBD model. A second-order polynomial model was utilized to estimate the OG dye removal as presented in the following Eq. (1).

$$Y = \beta_0 + \sum_{i=1}^{k} \beta_i \chi_i + \sum_{i=1}^{k} \beta_{ii} \chi_i^2 + \sum_{i=1}^{k} \sum_{j=1}^{k} \beta_{ij} \chi_i \chi_j + \varepsilon \quad (1)$$

where: Y represents the objective for optimizing the response. while k denotes the number of variables being considered. The indices i and j are used to represent the variable numbers. and $\beta 0$ is the constant coefficient. with βi and βii representing the linear and quadratic coefficients. respectively. The term βij refers to the interaction coefficient. and ε represents a random error. The values Xi and Xj correspond to the response of OG dye removal and

coded values for the independent factors (-1. 0. and +1). In the equation. a positive sign implies that the variables have a synergistic effect. whereas a negative sign indicates that they have an antagonistic effect.

Table 1. *Codes and actual variables and their levels in BBD.*

Codes	Variables	Level 1 (-1)	Level 2 (0)	Level 3 (+1)
A	CTS dose (g)	0.02	0.04	0.06
B	Contact time (min)	5	25	45
C	Temperature (°C)	30	45	60
D	Solution pH	4	7	10

To evaluate the precision of the model. the researchers employed Analysis of Variance (ANOVA) to examine the coefficients. The ANOVA provided several parameters. including *p*-value, *F*-value. determination coefficient (R^2), projected determination coefficient (R^2_{pred}). adjusted determination coefficient (R^2_{adj}), acceptable precision. degree of freedom (Df), and standard deviation (SD). The experimental data and model precision were evaluated using these parameters [21]. The researchers used a dependable second-order quadratic model equation to predict the optimal value and describe the interactions between the elements. To find the optimal values of the factors, they solved the regression equation. evaluated the counter-response surface map, and set limitations for the variable levels. To establish the extreme values of the variables. preliminary tests have been performed.

2.4. Batch Adsorption Study

The adsorption capacity of the CTS composite for the removal of OG dye was investigated using a batch system. A series of 250 mL Erlenmeyer flasks containing 100 mL of dye solution were employed, and a Box-Behnken Design (BBD) experimental methodology was applied to study the effects of key operational parameters. These parameters included the initial dye concentration (25–250 mg/L), adsorbent dosage (0.02–0.06 g), contact time (5–45 min), temperature (30–60 °C), and solution pH (4–10), as detailed in Table 2. Following the adsorption process, the adsorbent was separated from the solution either by centrifugation at 3400 rpm for 10 minutes. The residual dye concentration was then determined using a UV-Vis spectrophotometer (HACH DR 2800) at λ_{max} = 481 nm. The removal percentage (R. %) and the equilibrium adsorption capacity (qe. mg/g) were calculated by Eqs. (2), and (3).

$$R(\%) = \frac{C_0 - C_e}{C_0} \times 100 \quad (2)$$

$$q_e = \frac{V}{W}(C_0 - C_e) \quad (3)$$

Table 2*. Experimental matrix based on BBD approach for designing experiments and the corresponding response (OG removal).*

Run	A: CTS Dose (g)	B:Time (min)	C:Temp (°C)	D:pH	*OG removal* (%)
1	0.04	25	45	7	74.12
2	0.02	45	45	7	43.75
3	0.04	45	45	4	91.71
4	0.04	45	30	7	32.29
5	0.04	25	45	7	79.25
6	0.04	25	60	10	25.88
7	0.04	25	45	7	79.27
8	0.04	5	45	10	36.97
9	0.06	25	60	7	87.83
10	0.04	5	60	7	28.2
11	0.04	25	45	7	73.19
12	0.04	25	60	4	92.14
13	0.04	5	45	4	61.19
14	0.06	25	45	10	63.88
15	0.02	25	30	7	44.07
16	0.04	25	45	7	72.82
17	0.02	5	45	7	30.82
18	0.02	25	45	10	22.43
19	0.04	25	30	10	20.12
20	0.06	25	30	7	44.45
21	0.02	25	45	4	60.94
22	0.04	45	45	10	32.5
23	0.06	25	45	4	88.1
24	0.04	5	30	7	19.1
25	0.06	5	45	7	70.79
26	0.04	45	60	7	81.64
27	0.02	25	60	7	26.21
28	0.04	25	30	4	64.47
29	0.06	45	45	7	89.93

3. Results and discussion

3.1. Characterization of CTS

FTIR analysis was conducted on CTS before and after contact with OG dye solution, as shown in Fig. 2a-b, respectively. In Fig. 2a, the prominent peak at 3451 cm^{-1} is assigned to –OH and –NH groups. Asymmetric $–CH_2$ stretching appears as a strong band at 2920 cm^{-1}, Moreover, peaks at approximately 1381 cm^{-1} and 1416 cm^{-1} correspond to asymmetric deformation of $–CH_3$ in the amide group[22].The band at 1084 cm^{-1} reflects the skeletal vibrational stretch of C–O in the polysaccharide structure [13].

After OG dye adsorption onto the CTS surface (Fig. 2b), the amide bonds in chitosan exhibit characteristic absorbance at 1650 cm^{-1}, attributed to amide I (C=O) stretching. Additional changes include the appearance of an absorbance band at 1575 cm^{-1}, associated

with interactions involving C–N and C–N–H groups. The peak at 1416 cm^{-1}, corresponding to C–H bond interactions due to amide II, shows deformation after adsorption [23]. Moreover, the band at 1154 cm^{-1} indicates anti-symmetric C–O–C stretching [24]. These results meant that the CTS surface functional groups were successfully involved in the adsorption of OG dye.

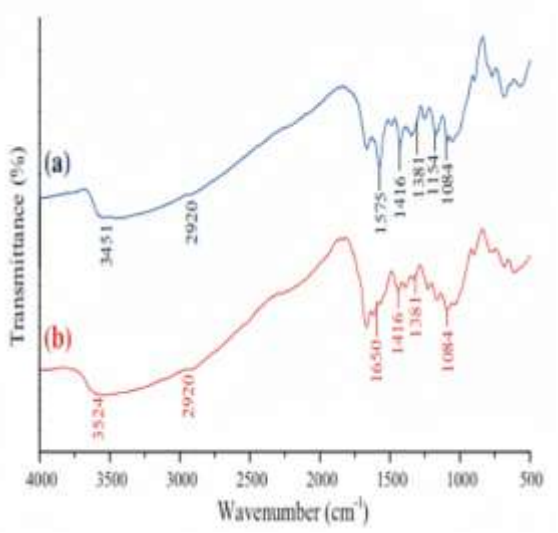

Figure. 2 *FTIR spectra of (a) CTS and (b) CTS after adsorption of OG dye.*

The surface morphology of CHB before and after OG dye adsorption is shown in Figs. 3a and 3b, respectively. As observed in Fig. 3a, the surface of CHB exhibits an irregular and heterogeneous structure with well-distributed cavities of varying sizes. These cavities provide favorable sites for enhanced adsorption of OG dye. This is further supported by Fig. 3b, which clearly shows a change in the CTS surface following dye adsorption, as evidenced by a denser morphology and a noticeable reduction in visible cavities.

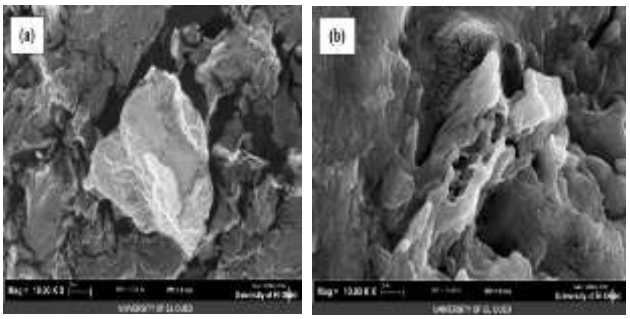

Figure. 3 *SEM images of (a) CTS and (b) CTS after OG dye adsorption.*

3.2. ANOVA analysis and BBD model fitting

The statistical significance of the BBD model was evaluated using analysis of variance (ANOVA). Table 3 presents the ANOVA results for the second-order response surface model. Model terms with Prob > F values less than 0.0500 indicate statistical significance under the selected experimental conditions. For the response variable (OG removal %), the significant model terms were identified as A, B, C, D, AC, BD, B^2, C^2, and D^2. In contrast, the terms AB, AD, BC, CD, and A^2 showed lower significance and could be omitted to refine the model. Accordingly, the reduced model is represented by the following second-order polynomial equation (Eq. (4)):

$$\text{OG removal (\%)} = +75.73 + 18.06A + 10.39B + 9.78C - 21.39D + 15.31AC - 8{,}74BD - 12.97B^2 - 19.54C^2 - 7.79D^2 \quad (4)$$

The individual effect of the studied variables including adsorbent dose (A), time (B), temperature (C), and pH (D) and removal efficiency (%) was investigated by perturbation plots as shown in Fig. 4.a. The steep curvature in the profile of factor A (adsorbent dose) indicates that the removal process is highly sensitive to this variable. Similarly, the relatively sharp slope of factor C (temperature) demonstrates a significant sensitivity to changes in operating temperature. In contrast, the curve for factor D (pH) exhibits a slow curvature, suggesting that this factor has a slight effect on the response.

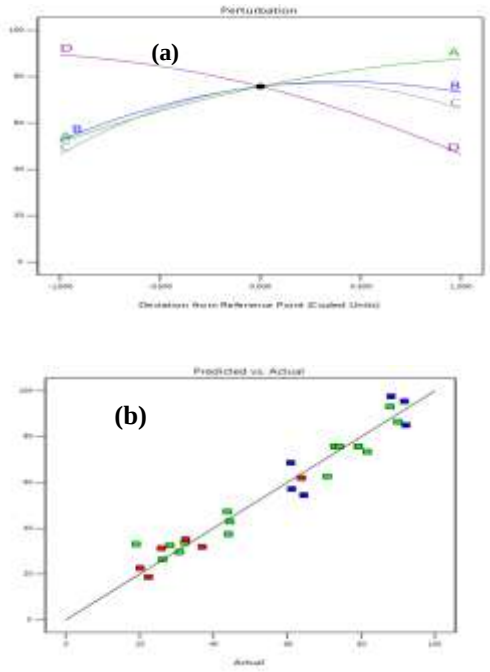

Figure. 4 *(a) Perturbation plots for the removal of OG using CTS, (b) plot of the relationship between the theoretical and real values of OG dye.*

From Fig. 4.a, it can be seen that the OG dye color removal efficiency increases as the adsorbent dosage increases, while it tends to decrease as the pH increases. The goodness of fit of the model was also

tested by the multiple correlation coefficients (R^2). In this case, the value of the multiple correlation coefficients was 0.9487, which implied that this regression is statistically significant. This can be observed in Fig. 4.b by comparing the actual values against the predicted responses by the model for the percentage of OG dye removal. The value of predicted multiple correlation coefficient (pred. R^2 = 0.7146) is in reasonable agreement with the value of the adjusted multiple correlation coefficient (adj. R^2 = 0.8974). This pattern confirms the absence of systematic bias and validates the model's fit to the experimental data. Furthermore, the close correlation between actual and predicted removal efficiencies for OG dye (Fig. 4b) underscores the model's accuracy and predictive reliability [25].

3.3. Significant interactions

The significance of variable interactions was evaluated using Table 3. A statistically significant interaction was found between CTS dose (A) and temperature (C), with a p-value of 0.0019, while other variables (contact time at 25 min, pH ~4) were simultaneously kept constant within the experimental range.

Table 3. *Analysis of variance (ANOVA) for OG removal (%).*

Source	Sum of Squares	Df	Mean Square	F-value	p-value
Model	16791,43	14	1199,39	18,50	< 0.0001
A-Dose	3915,41	1	3915,41	60,38	< 0.0001
B-Time	1296,88	1	1296,88	20,00	0,0005
C-Temp	1148,56	1	1148,56	17,71	0,0009
D-pH	5494,24	1	5494,24	84,73	< 0.0001
AB	9,64	1	9,64	0,1487	0,7056
AC	937,58	1	937,58	14,46	0,0019
AD	51,05	1	51,05	0,7873	0,3899
BC	405,02	1	405,02	6,25	0,255
BD	306,08	1	306,08	4,72	0,0475
CD	120,01	1	120,01	1,85	0,1952
A^2	248,57	1	248,57	3,83	0,0705
B^2	1092,71	1	1092,71	16,85	0,0011
C^2	2476,72	1	2476,72	38,20	< 0.0001
D^2	394,55	1	394,55	6,08	0,0272
Residual	907,79	14	64,84		
Lack of Fit	865,36	10	86,54	8,16	0,0289
Pure Error	42,43	4	10,61		
Cor Total	17699,22	28			

This interaction is visualized in the 3D response surface plots in Fig. 5.a. Increasing the adsorbent dose from 0.02 g to 0.06 g enhanced OG dye removal, likely due to greater surface area and active sites. Temperature, however, showed no significant effect on removal, indicating an endothermic adsorption process, which will be discussed in Section 3.7.

The interaction between contact time (B) and solution pH (D) significantly affected OG dye removal (p = 0.0475), with adsorbent dose (0.06 g) and temperature (60°C) held constant. The 3D response surface in Fig. 5b illustrates this interaction. Reducing the pH from 4 to 10 increased dye removal from 19.1% to 92.14 %. The pH_{pzc} of the CTS composite was 7.5 (Fig. 5c), indicating a cationic surface due to amino groups ($-NH_3^+$). Below this pH, the positively charged surface enhances anionic OG dye adsorption via electrostatic attraction between $-NH_3^+$ and dye sulfonate groups ($-SO_3^-$), a mechanism consistent with prior research [26]. Therefore, pH 4.0 was established as the optimal condition to exploit this protonation-enhanced adsorption. as described by Eq. (5).

$$R\text{-}NH_3^+ + OG\text{-}SO_3^- \leftrightharpoons R\text{-}NH_3^+ \text{---} O_3S\text{--}OG \quad (5)$$

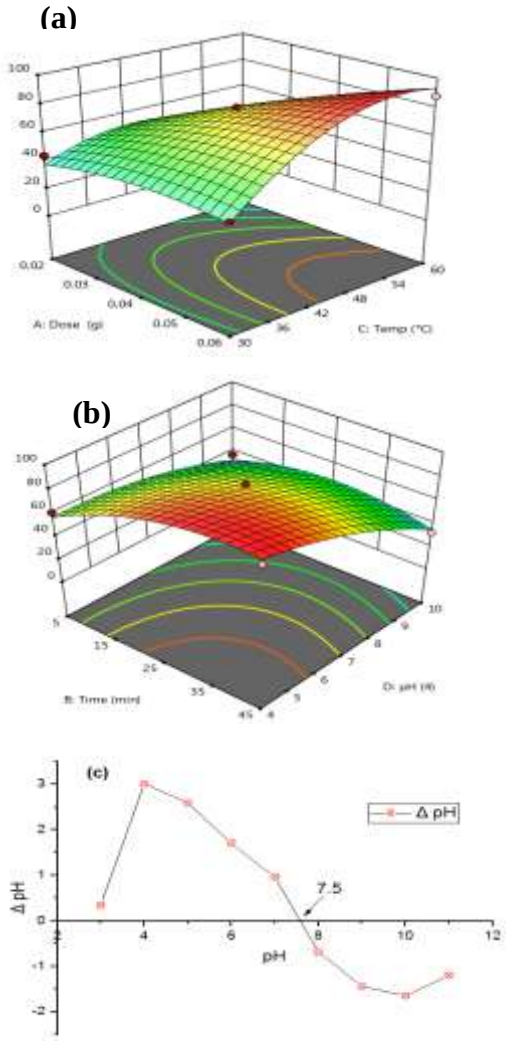

Figure. 5 *3D response surfaces plots of significant interactions on color removal of OG dye: (a) for BC interaction; (b) for AC interaction; whereas (c) pH_{pzc} of CTS.*

3.4. Adsorption Study

The influence of contact time on the adsorption of OG dye onto the CTS surface was examined at various initial dye concentrations (25 to 200 mg/L), while maintaining constant conditions including an adsorbent dose of 0.04 g/100 mL, solution pH 4, and temperature of 60 °C. Fig. 6 illustrates the adsorption capacity (qt, mg/g) of CTS over time for each initial dye concentration. As shown, the adsorption capacity increased from 56.13 to 153.38 mg/g as the initial OG concentration rose from 25 to 200 mg/L. This trend can be attributed to the enhanced concentration gradient at higher dye concentrations, which facilitates greater diffusion of OG dye molecules into the internal pores of the adsorbent and promotes their migration to active adsorption sites [8, 27]

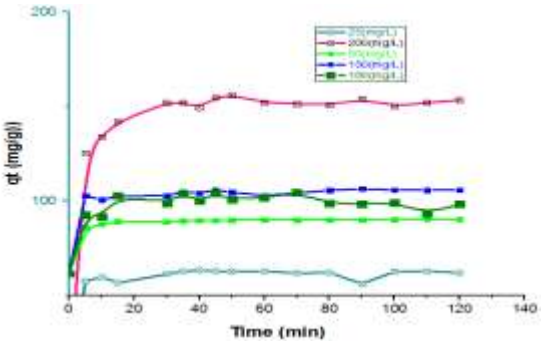

Figure. 6*. Effect of the contact time on OG adsorption at different initial concentrations by CTS (adsorbent dose = 0.04 g, temperature = 60 °C solution pH =4, and volume of solution = 100 mL).*

3.5 Adsorption kinetics

To further elucidate the adsorption behavior and underlying mechanism of OG dye onto the CTS surface, the kinetic data were analyzed using two commonly applied models: the pseudo-first-order (PFO) and pseudo-second-order (PSO) kinetic models [28, 29]. These models are essential for understanding the rate-controlling steps and the nature of the adsorption process, whether it involves physical or chemical interactions. The nonlinear expressions of the PFO and PSO models are given in Eqs. (6) and (7), respectively.

$$\ln(q_e - q_t) = lnq_e - K_1 \quad (6)$$

$$\frac{t}{q_t} = \frac{1}{q_e^2 K_2} + \frac{t}{q_e} \quad (7)$$

where: q_t is the observed adsorption capacity at time t, and k_1 and k_2 are the rate constants for PFO (min^{-1}) and PSO ($g.mg^{-1}.min^{-1}$), respectively.

The kinetic parameters for the adsorption of OG dye onto the CTS surface are summarized in Table 4. As shown, the pseudo-second-order (PSO) model yielded R^2 values closer to unity compared to the pseudo-first-order (PFO) model.

Furthermore, upon comparison of the modeling results, the PSO model demonstrated a better fit with the experimental data, as the calculated adsorption capacities (qe,cal) closely matched the experimental values ($q_{e,exp}$). This strong correlation suggests that the adsorption of OG dye onto CTS primarily follows a chemisorption mechanism [30].

Table 4. *PFO and PSO kinetic parameters for OG dye adsorption on CTS*

Concentration (mg/L)		25	50	100	150	200
$q_{e\,exp.}$ (mg/g)		62.55	124.58	153.38	178.38	185.71
PFO	$q_{e\,cal}$ (mg/g)	62.18	119.33	143.21	177.68	183.09
	k_1 (1/min)	0.4031	0.2073	0.0313	0.0274	0.2456
	R^2	0.999	0.997	0.973	0.999	0.999
PSO	$q_{e\,cal}$ (mg/g)	62.50	125.00	153.85	178.57	185.19
	$k_2 \times 10^{-2}$ (g/mg min)	0.952	0.610	0.454	2.509	0.164
	R^2	0.996	0.999	0.999	0.998	0.991

3.6 Adsorption isotherms

The adsorption equilibrium data for OG dye on CTS were modeled using three common isotherms: Langmuir [31], Freundlich [32], and Temkin [33]. This analysis is crucial for understanding the adsorbent-adsorbate interactions and for calculating the maximum adsorption capacity. The corresponding non-linear equations for these models are given in Eqs. (8)–(10).

$$q_e = \frac{q_{max} K_L C_e}{1 + K_L C_e} \quad (8)$$

$$q_e = K_F C_e^{1/n} \quad (9)$$

$$q_e = \left(\frac{RT}{b_T}\right) ln(K_T C_e) \quad (10)$$

where: K_L is the Langmuir constant ($L.mg^{-1}$), and q_{max} is the maximum monolayer adsorption capacity ($mg.g^{-1}$), K_F is the Freundlich constant ($mg.g^{-1}.mg^{-1/n}.L^{-1/n}$), and n is the Freundlich constant related to adsorption intensity, K_T is the Temkin constant ($L.g^{-1}$), b_T is the equilibrium binding constant ($J.mol^{-1}$), R is the ideal gas constant (8.314 $J.mol^{-1}.K^{-1}$), and T is the absolute temperature (K).

The plots of the non-linear forms of the studied models are presented in Fig. 7, and their corresponding values of isotherm parameters are given in Table 5. It can be noticed from the (R^2 = 0.995) that the Langmuir model obviously shows the best fitting for the isotherm data, suggesting the uniform monolayer adsorption of OG molecules occurs on the CTS surface [34]. The q_{max} for the CTS was calculated to 416.67 mg/g (see Table 5) based on the Langmuir model.

Table 5. *Parameters of the Langmuir, Freundlich and Temkin isotherm models for OG dye adsorption on CTS at 60 °C.*

Adsorption isotherm	Parameter	Value
Langmuir	q_{max} (mg/g)	416.67
	K_a (L/mg)	0.026
	R^2	0.984
Freundlich	K_f (mg/g) $(L/mg)^{1/n}$	32.97
	n	2.16
	R^2	0.99
Temkin	K_T (L/mg)	0.465
	b_T (J/mol)	34.68
	R^2	0.946

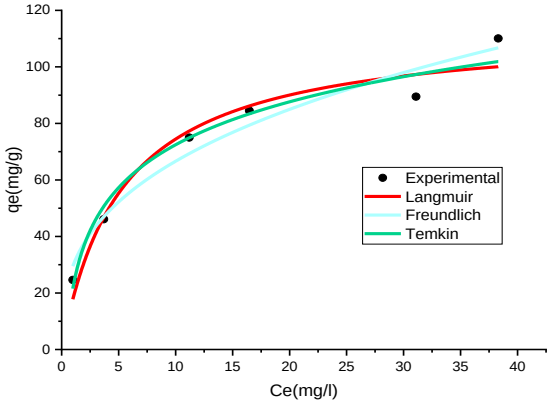

Figure. 7*. Adsorption isotherms of OG by CTS (adsorbent dose = 0.04 g, solution pH =4, temperature = 60 °C, and volume of solution = 100 mL).*

The comparison of the adsorption capacity of CTS with other adsorbents used for OG adsorption is shown in Table 6. As recorded in Table 6, CTS introduces itself as a promising and efficient adsorbent for the color removal of reactive dyes from contaminated water.

Table 6. *Comparison of the adsorption capacities of OG dye by various adsorbents.*

Adsorbents	q_{max} (mg/g)	References
Chitosan (CTS)	416.67	Present work
Alumina nanoparticle	93.3	[35]
Chitosan/activated carbon/polyaniline (AC@chitosan@PANI)	112	[36]
Zinc oxide activated carbon (ZnO-AC)	153.8	[37]
Montmorillonite modified with CTAB	167	[38]
Cross-linked chitosan-glutaraldehyde	206.65	[39]
Activated Bentonite - CTAB	102.80	[40]

3.7. Adsorption thermodynamics

The thermodynamics of OG dye adsorption on the CTS surface were investigated to determine the process feasibility, spontaneity, and the level of disorder at the adsorbent-adsorbate interface. The standard Gibbs free energy change (ΔG°), enthalpy change (ΔH°), and entropy change (ΔS°) were determined according to Eqs. (11)–(13) [41, 42].

$$\ln k_d = \frac{\Delta S^\circ}{R} - \frac{\Delta H^\circ}{RT} \quad (11)$$

$$k_d = \frac{Q_e}{C_e} \quad (12)$$

$$\Delta G^\circ = -RT \ln k_d \quad (13)$$

The values of ΔH° and ΔS° were determined from the slope and intercept, respectively, of the van't Hoff plot (ln K_d vs. 1/T), as presented in Fig. 8

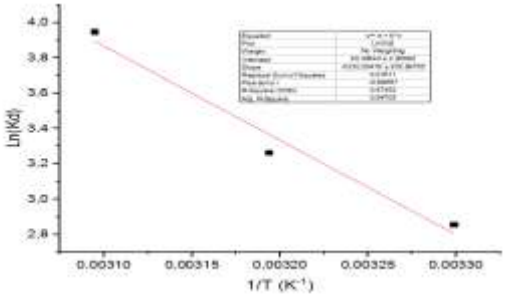

Figure. 8*. Van't Hoff plot for OG by CTS (adsorbent dose = 0.06 g. solution pH =4. temperature = 45 °C. and volume of solution = 100 mL).*

From the results presented in Table 7, the negative ΔG° values validates that the adsorption of OG dye onto the CTS was a spontaneous and favorable process [43]. The positive value of ΔS° points the increasing in irregularity during OG dye adsorption on the CTS surface. Whereas the positive value of ΔH° reflects that the OG dye adsorption process was endothermic in nature. Moreover, the increasing in adsorption capacity of CTS at high temperature can be attributed to the effect of temperature on the internal structure of the CTS, thus facilitate faster diffusion of OG dye molecules into the CTS's interspaces structure [8, 44].

Table 7. *Thermodynamic parameters for the adsorption of OG dye on CTS*

T(K)	Ln K_d	ΔG° (kJ/mol)	ΔH° (kJ/mol)	ΔS°(kJ/mol K)
303,15	-0.14	-7.20	44.31	0.168
313.15	0.806	-8.50		
318.15	1.752	-10.61		
333.15	2.699	-10.93		

4. Conclusions

In this work, chitosan powder was converted into beads form and successful study was completed for the adsorption of OG dye from aqueous solution. The optimum experimental conditions for OG dye

by BBD-RSM were recorded at solution pH 4, CTS dose (0.04 g/L), and time (25 min). The results indicate that the highest OG dye removal (92.14 %) were observed at the following significant interactions: AC (CTS dose ×temperature) and BD (time×pH). The desirable adsorption capacity of 416.67 mg/g for OG dye by CTS was obtained at 60 °C. The equilibrium and kinetics data exposed that the OG dye adsorption was chemisorption and monolayer on the surface of CTS. Thermodynamics calculation denotes that the adsorption process was spontaneous and endothermic in nature. This work elucidates that CTS composite has great potential as a low-cost and effective adsorbent for the organic dyes removal and water/wastewater.

Author Statements:

- **Ethical approval:** The conducted research is not related to either human or animal use.
- **Conflict of interest:** The authors declare that they have no known competing financial interests or personal relationships that could have appeared to influence the work reported in this paper
- **Acknowledgement:** The authors express their gratitude to the General Directorate of Scientific Research and Technological Development in Algeria for their provision of laboratory facilities.
- **Author contributions:** All authors contributed to the study conception and design. Material
- **Funding information**: The authors declare that there is no funding to be acknowledged.
- **Data availability statement**: The data that support the findings of this study are available on request from the corresponding author. The data are not publicly available due to privacy or ethical restrictions.

References

[1] A. Hamidi, D. Atia, A. Rebiai, A. Reghioua, A. Zobeidi, M. Messaoudi, *et al.*, "Investigation of adsorption kinetics and isothermal thermodynamics for optimizing methylene blue adsorption onto a modified clay with cellulose using the response surface approach," *Biomass Conversion and Biorefinery*, vol. 14, pp. 22573-22587, 2024.

[2] M. Liaqat, R. R. M. Khan, T. Iqbal, and X.-Z. Fu, "Introduction to Dyes," 2025.

[3] A. H. Jawad, N. S. A. Mubarak, and A. S. Abdulhameed, "Hybrid crosslinked chitosan-epichlorohydrin/TiO2 nanocomposite for reactive red 120 dye adsorption: kinetic, isotherm, thermodynamic, and mechanism study," *Journal of Polymers and the Environment*, vol. 28, pp. 624-637, 2020.

[4] A. Zobeidi and L. Moussaoui, "Physico-chemical quality of drinking water in the south of Algeria (Case of El-Oued region) study of excess minerals," *International Letters of Chemistry, Physics and Astronomy*, vol. 11, 2013.

[5] S. Bahemmi, A. Zobeidi, S. Atia, S. Neghmouche Nacer, D. Ghernaout, and N. Elboughdiri, "Activating illite kaolinite clay with CTAB for adsorbing methylene blue: isotherms, kinetics, and thermodynamics studies," *Tuijin Jishu/Journal of Propulsion Technology*, vol. 44, p. 2023, 2023.

[6] N. Y. Donkadokula, A. K. Kola, I. Naz, and D. Saroj, "A review on advanced physico-chemical and biological textile dye wastewater treatment techniques," *Reviews in environmental science and bio/technology*, vol. 19, pp. 543-560, 2020.

[7] D. Atia, A. A. Bebba, L. Haddad, and A. Zobeidi, "Elimination of organic pollutants from urban wastewater by illite-kaolinite local clay from south-east of Algeria," *Cienc. Tecn. Vitivinic*, vol. 33, pp. 17-28, 2018.

[8] D. Atia, A. Zobeidi, S. Neghmouche Nacer, D. Ghernaout, and N. Elboughdiri, "Biocomposite of nontronite/Enteromorpha sp. for cationic methylene blue dye removal: optimization, kinetics, and isothermal thermodynamics study," *Biomass Conversion and Biorefinery*, vol. 15, pp. 13347-13364, 2025.

[9] D. Atia, A. Kamarchou, and A. Zobeidi, "Removal of organic pollutants from wastewater by activated carbon prepared from dates stones of Southern Algeria," *Journal of Fundamental and Applied Sciences*, vol. 12, pp. 230-241, 2020.

[10] R. R. Mohamed, "Chitin and chitosan as adsorbents," in *Natural Polymers-Based Green Adsorbents for Water Treatment*, ed: Elsevier, 2021, pp. 73-91.

[11] W. Al-Gethami, M. A. Qamar, M. Shariq, A.-N. M. Alaghaz, A. Farhan, A. A. Areshi, *et al.*, "Emerging environmentally friendly bio-based nanocomposites for the efficient removal of dyes and micropollutants from wastewater by adsorption: a comprehensive review," *RSC advances*, vol. 14, pp. 2804-2834, 2024.

[12] K. Wang, P. Wu, Z. Hu, and X. D. Chen, "pH-Sensitive, Edible Chitosan-Based Hydrogels with Extremely High Swelling and Reinforced Mechanics: A Chemical-Free Crosslinking Strategy for Gastric Retention," *Food Hydrocolloids*, p. 111654, 2025.

[13] Q. Li, E. Dunn, E. Grandmaison, and M. F. Goosen, "Applications and properties of chitosan," in *Applications of Chitan and Chitosan*, ed: CRC Press, 2020, pp. 3-29.

[14] H. Alzain, V. Kalimugogo, K. Hussein, and M. Karkadan, "A review of environmental impact of azo dyes," *Int J Res Rev*, vol. 10, pp. 673-689, 2023.

[15] N. d. C. L. Beluci, G. A. P. Mateus, C. S. Miyashiro, N. C. Homem, R. G. Gomes, M. R. Fagundes-Klen, *et al.*, "Hybrid treatment of coagulation/flocculation process followed by ultrafiltration in TIO2-modified membranes to improve the removal of reactive black 5 dye," *Science of the Total Environment*, vol. 664, pp. 222-229, 2019.

[16] A. H. Jawad, N. N. A. Malek, A. S. Abdulhameed, and R. Razuan, "Synthesis of magnetic chitosan-fly ash/Fe3O4 composite for adsorption of reactive orange 16 dye: optimization by Box–Behnken

design," *Journal of Polymers and the Environment*, vol. 28, pp. 1068-1082, 2020.

[17] P. Sharma, H. Kaur, M. Sharma, and V. Sahore, "A review on applicability of naturally available adsorbents for the removal of hazardous dyes from aqueous waste," *Environmental monitoring and assessment*, vol. 183, pp. 151-195, 2011.

[18] S. Nayak, P. Krishna, B. Dey, A. Lal, and S. Dey, "Chitosan-based adsorbents for the decontamination of pollutants from water and regeneration study of spent adsorbents: a critical review," *Journal of the Iranian Chemical Society*, vol. 23, p. 35, 2026.

[19] W. W. Ngah, M. Hanafiah, and S. Yong, "Adsorption of humic acid from aqueous solutions on crosslinked chitosan–epichlorohydrin beads: Kinetics and isotherm studies," *Colloids and Surfaces B: Biointerfaces*, vol. 65, pp. 18-24, 2008.

[20] L. Miao, L. Hu, X. Mao, R. Yang, Z. Hong, J. Zhao, *et al.*, "Epichlorohydrin cross-linked chitosan for adsorption of reactive red 2 dye: Optimization and adsorption mechanism," *International Journal of Biological Macromolecules*, vol. 320, p. 146202, 2025.

[21] J. Cornell and R. Berger, "Factors that influence the value of the coefficient of determination in simple linear and nonlinear regression models," *Phytopathology*, vol. 77, pp. 63-70, 1987.

[22] R. Rusmin, B. Sarkar, Y. Liu, S. McClure, and R. Naidu, "Structural evolution of chitosan–palygorskite composites and removal of aqueous lead by composite beads," *Applied Surface Science*, vol. 353, pp. 363-375, 2015.

[23] E. Güzelyurt, A. Kolburan Geçer, A. Deveci Topal, and C. Dilek Eren, "Examination of student perceptions of asynchronous learning environments within the framework of technology acceptance model," *The International Journal of Information and Learning Technology*, pp. 1-14, 2026.

[24] D. M. Mamand, J. M. Hadi, R. A. Omer, and S. B. Aziz, "FTIR, UV-VIS, and DFT approach to study the structural, optical and thermal properties of Chitosan biopolymer," in *Doklady Physical Chemistry*, 2024, pp. 137-154.

[25] S. M. Haque, T. N. Aldhafeeri, N. Rahman, R. Jain, Y. Umar, and M. R. Siddiqui, "The application of Box-Behnken-Design in the optimization of kinetic spectrophotometry and computational studies to determine and assessing eco-scale to green analytical chemistry for labetalol," *Journal of Pharmaceutical Innovation*, vol. 19, p. 28, 2024.

[26] W. A. Al-Amrani, M. A. K. M. Hanafiah, and A.-H. A. Mohammed, "A comprehensive review of anionic azo dyes adsorption on surface-functionalised silicas," *Environmental Science and Pollution Research*, vol. 29, pp. 76565-76610, 2022.

[27] A. Rana and K. Qanungo, "Orange G dye removal from aqueous-solution using various adsorbents: A mini review," *Materials Today: Proceedings*, vol. 81, pp. 754-757, 2023.

[28] S. Lagergren, "Zur theorie der sogenannten adsorption geloster stoffe," 1898.

[29] Y.-S. Ho and G. McKay, "Sorption of dye from aqueous solution by peat," *Chemical engineering journal*, vol. 70, pp. 115-124, 1998.

[30] A. D. Khatibi, M. Yilmaz, A. H. Mahvi, D. Balarak, and S. Salehi, "Evaluation of surfactant-modified bentonite for Acid Red 88 dye adsorption in batch mode: Kinetic, equilibrium, and thermodynamic studies," *Desalination and Water Treatment*, vol. 271, pp. 48-57, 2022.

[31] I. Langmuir, "The adsorption of gases on plane surfaces of glass, mica and platinum," *Journal of the American Chemical society*, vol. 40, pp. 1361-1403, 1918.

[32] H. Frundlich, "Adsorption in solution," *Z. Phys. Chem*, vol. 57, pp. 384-470, 1906.

[33] M. Temkin, "Kinetics of ammonia synthesis on promoted iron catalysts," *Acta physiochim. URSS*, vol. 12, pp. 327-356, 1940.

[34] K. Yokwana, A. T. Kuvarega, S. D. Mhlanga, and E. N. Nxumalo, "Mechanistic aspects for the removal of Congo red dye from aqueous media through adsorption over N-doped graphene oxide nanoadsorbents prepared from graphite flakes and powders," *Physics and Chemistry of the Earth, Parts A/B/C*, vol. 107, pp. 58-70, 2018.

[35] S. Banerjee, S. Dubey, R. K. Gautam, M. Chattopadhyaya, and Y. C. Sharma, "Adsorption characteristics of alumina nanoparticles for the removal of hazardous dye, Orange G from aqueous solutions," *Arabian Journal of Chemistry*, vol. 12, pp. 5339-5354, 2019.

[36] A. Grich, T. Bouzid, A. Naboulsi, H. Yazid, A. Regti, M. El Himri, *et al.*, "Synthesis of a novel hierarchical adsorbent AC@ chitosan@ PANI for removal of orange G: Synergistic effects, statistical physics modeling, and adsorption mechanism," *Journal of Molecular Liquids*, p. 129253, 2026.

[37] J. Saini, V. Garg, R. Gupta, and N. Kataria, "Removal of Orange G and Rhodamine B dyes from aqueous system using hydrothermally synthesized zinc oxide loaded activated carbon (ZnO-AC)," *Journal of environmental chemical engineering*, vol. 5, pp. 884-892, 2017.

[38] H. Ouachtak, A. El Guerdaoui, R. Haounati, S. Akhouairi, R. El Haouti, N. Hafid, *et al.*, "Highly efficient and fast batch adsorption of orange G dye from polluted water using superb organo-montmorillonite: Experimental study and molecular dynamics investigation," *Journal of Molecular Liquids*, vol. 335, p. 116560, 2021.

[39] A. Amjlef, S. Farsad, A. Chaoui, A. B. Hamou, M. Ezzahery, S. Et-Taleb, *et al.*, "Effective adsorption of Orange G dye using chitosan cross-linked by glutaraldehyde and reinforced with quartz sand," *International Journal of Biological Macromolecules*, vol. 239, p. 124373, 2023.

[40] Z. Taibi, K. Bentaleb, Z. Bouberka, C. Pierlot, M. Vandewalle, C. Volkringer, *et al.*, "Adsorption of orange G dye on hydrophobic activated bentonite from aqueous solution," *Crystals*, vol. 13, p. 211, 2023.

[41] S. Mabrouk, A. A. Bebba, A. Kamarchou, and A. Zobeidi, "Adsorption capacity of pollutants by using local clay mineral from urban wastewater Touggourt (South-East Algeria)," *Asian Journal of Research in Chemistry*, vol. 13, pp. 85-90, 2020.

[42] B. Assia, H. Zaghouane-Boudiaf, R. Bourzami, F. Djerboua, B. Hameed, and M. Boutahala, "Cross-linked chitosan-epichlorohydrin/bentonite composite for reactive orange 16 dye removal: Experimental study and molecular dynamic simulation," 2023.

[43] J. Liu, X. Yang, H. Liu, W. Cheng, and Y. Bao, "Modification of calcium-rich biochar by loading Si/Mn binary oxide after NaOH activation and its adsorption mechanisms for removal of Cu (II) from aqueous solution," *Colloids and Surfaces A: Physicochemical and Engineering Aspects*, vol. 601, p. 124960, 2020.

[44] R. Mecheri, A. Zobeidi, S. Atia, S. Neghmouche Nacer, A. A. Salih, M. Benaissa, *et al.*, "Modeling and optimizing the crystal violet dye adsorption on kaolinite mixed with cellulose waste red bean peels: insights into the kinetic, isothermal, thermodynamic, and mechanistic study," *Materials*, vol. 16, p. 4082, 2023.